

Ferromagnetism in Cr-doped In_2O_3 revisited

Paola Alippi,¹ Maura Cesaria,² and Vincenzo Fiorentini^{3,4}

¹*CNR-ISM, Via Salaria, Km 29.300, I-00016 Monterotondo Scalo, Rome, Italy*

²*Dipartimento di Matematica e Fisica, Università del Salento, Via Arnesano, I-73100 Lecce, Italy*

³*Dipartimento di Fisica, Università di Cagliari, Cittadella Universitaria, Monserrato, I-09042 Cagliari, Italy*

⁴*CNR-IOM, UOS Cagliari, Cittadella Universitaria, Monserrato, I-09042 Cagliari, Italy*

(Dated: August 16, 2022)

The origin of ferromagnetism in Cr-doped In_2O_3 is re-examined using state-of-the-art hybrid density-functional calculations. We show that the electronic structure of isolated Cr is not compatible with ferromagnetism, and propose an alternative mechanism, based on the pairing of Cr and oxygen vacancies and boosted by intentional doping, which is consistent with experimental results such as the onset of ferromagnetism only in O-lean conditions, the low or vanishing net moment in unintentionally doped material, and its increase upon intentional doping.

PACS numbers: 75.50.Pp,71.55.-i,71.15.Mb,61.72.Bb

Transparent conducting oxides are a key part of modern electronic technology, and the addition of permanent magnetism to their functionalities is a potentially momentous breakthrough. Cr-doped indium oxide ($\text{Cr}:\text{In}_2\text{O}_3$) has been reported [1, 2] to be a ferromagnet (FM) with above-room-temperature Curie point, typically in O-lean preparation conditions and with FM progressively stabilizing as the carrier concentration is increased. A diluted-magnetic-semiconductor-like [3] theoretical picture [4, 5] suggest that FM coupling is due to extrinsic (i.e. provided by doping or defects) carriers populating spin-polarized Cr-induced levels resonant with the host conduction band.

In this Letter we reconsider magnetism in $\text{Cr}:\text{In}_2\text{O}_3$ using hybrid density-functional theory (DFT), one of the current cutting-edge ab initio theoretical approaches to materials. The results suggest that spin-polarized states of isolated Cr are inaccessible to doping, essentially barring itinerant magnetic coupling. We propose the $\text{Cr}-\text{V}_\text{O}$ complex as an alternative magnetic-doping unit; its electronic structure and properties match, among others, the strong experimental indications that FM is achieved in O-deficient conditions.

The key ingredient of a theoretical discussion of magnetic coupling between Cr impurities is an accurate description of the position of Cr-induced states relative to the bulk bands edges of In_2O_3 , which of course should also be accurately described. This is a contentious point in ab initio density-functional theory (DFT) defects calculations, especially those based on semilocal functionals such as the local (LDA) and gradient-corrected (GGA) approximations, which underestimate the fundamental gap and may misplace the extrinsic levels within the host band structure. Indeed, in the current picture [6] of $\text{Cr}:\text{In}_2\text{O}_3$, semilocal density functionals had to be supplemented with a combination of empirical non-local potentials (NLEP) and “+U” corrections on In and Cr d -states. To cure the drawbacks (gap underestimate, etc.) of semilocal functionals, here we use instead the Heyd-

Scuseria-Ernzerhof (HSE) hybrid exchange-correlation functional [7], a Perdew-Burke-Ernzerhof [8] GGA functional modified to include a fraction α_{HF} of non-local short-range Hartree-Fock (HF) exact exchange, screened by a model dielectric function over a characteristic wave-vector μ (fixed in this work to a standard 0.2 \AA^{-1}). The use of this technique is becoming increasingly common for defects in semiconductors [9, 10]. The standard solid-state recipe (the HSE06 functional) is $\alpha_{\text{HF}}=0.25$, but we examine the In_2O_3 gap and the Cr levels position as function of the mixing parameter α_{HF} in the range $0 \div 0.3$. This is necessary as that position affects directly the interpretation of FM, and on the other hand it cannot be confidently assessed experimentally.

We perform collinear spin-polarized total-energy, force, and band calculations for In_2O_3 in various states (undoped, Cr- and Sn-doped, O-deficient, and containing Cr-O vacancy complexes) with the hybrid HSE06 functional and the projector augmented wave (PAW) method [11] as implemented in the VASP code [12]. We use an energy cutoff of 500 eV, a Γ -centered $2 \times 2 \times 2$ Monkhorst-Pack k -points grid, and treat In $4d$ and Cr $3d$ states as valence. All calculations are done at the experimental [13] lattice constant $a_{\text{eq}}=10.12 \text{ \AA}$ with an upper threshold of 0.02 eV/\AA on Hellmann-Feynman forces. For $\alpha_{\text{HF}}=0.25$ the Kohn-Sham band gap (valence band maximum (VBM) to conduction band minimum (CBM)) of bulk In_2O_3 is 2.9 eV, direct at Γ , as in other HSE06 calculations [14], and close to the experimentally reported 2.9 eV [15]. The valence band is dominated by O $2p$ states and $\simeq 6 \text{ eV}$ wide as in experiment [16], while the CBM is free electron-like and of mainly In $5s$ character. The centroid of In $4d$ states is 13.5 eV below the VBM, close to 14 eV experimentally [17]. Thus, the HSE electronic structure of undoped In_2O_3 is a good starting point for the study of the electronic structure of the Cr-doped system.

Bulk In_2O_3 has the bixbyite structure (group T_h) often adopted by sesquioxides [18], with a 40-atom primitive cell consisting of a collection of fluorite-structure cells

each missing two O atoms and appropriately rotated relative to one another. O's are fourfold coordinated with four different distances to their neighbors. Cations are six-fold coordinated and occupy the Wyckoff [20] sites $8b$ and $24d$ which we refer to below as b and d . The b cations have six neighboring O's at the same distance, the d ones have three pairs of neighboring O's at three distinct (though similar) distances.

The isolated Cr impurity replaces one In atom at either the b or the d site in a doubled cell (80 atoms), i.e. the Cr density is 3.1%. In both cases, the Cr-O bonds are shorter ($\simeq -7\%$) than In-O bonds. The higher-symmetry b -site is the favored site for Cr, with the d site 55 meV higher in energy.

As expected from its nominally trivalent oxidation, Cr induces no near-edge donor or acceptor-like state. In the majority channel, a triplet of occupied Cr levels sits near the VMB (i.e. about 2.5 eV below the CBM) and a doublet of empty states is about 2.5 eV above the CBM; in the minority channel, only unoccupied Cr-related states appear, at 3 eV above the CBM. t_{2g} -like Cr states are lower than e_g -like states as expected in an octahedral crystal field. The majority t_{2g} triplet is occupied, while majority e_g and minority t_{2g} and e_g states are empty. Below we concentrate on the energetically-favored Cr_b site, but Cr_d has essentially identical levels, aside from small degeneracy lifting due to its lower symmetry.

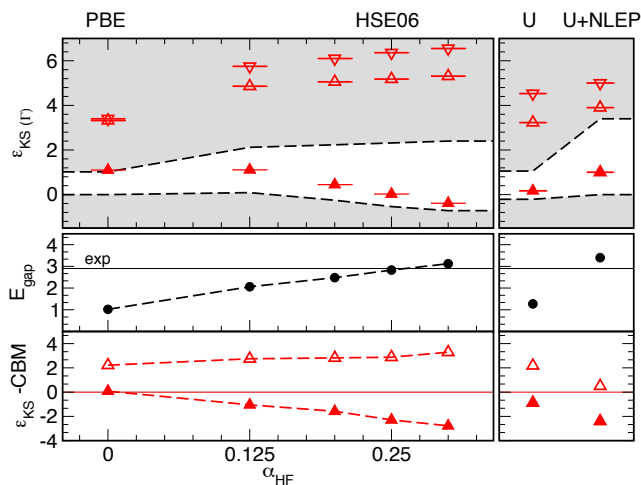


FIG. 1. (Color online) Left panel, levels as function of α_{HF} : Cr_b levels within the In_2O_3 bands referred to valence band edge (top); In_2O_3 band gap (center); last occupied and first empty Cr_b states (bottom) referred to CBM. Right panel: same quantities as left panel in GGA+U ($U_{\text{In}}=4.5$ eV, $U_{\text{Cr}}=2$ eV) and in GGA+U/NLEP (Ref.5). Legend: majority (minority) states are up (down) triangles, occupied (empty) states are filled (empty) triangles. Black circles are gap values. All energies are in eV.

The energy location of Cr-levels with respect to band edges is crucial to carrier-mediated FM.[19] It is currently thought that Cr levels adjacent to the CBM can be occu-

ried by extrinsic carriers, producing coupling of dilute Cr centers. However, with HSE06 we find no Cr levels accessible to doping in the vicinity of the band edges. We thus monitor the effects on impurity levels of the corrections provided by HSE over GGA (mostly, self-interaction removal and non-locality) as determined by the fraction α_{HF} of exact exchange in the hybrid functional. We perform structural optimization and electronic structure calculations for Cr_b for $\alpha_{\text{HF}}=0$ to 0.3, summarized in Fig.1 (energies are taken at the Γ point).

As expected, the hybrid functional opens up the band gap nearly linearly in α_{HF} and matches experiment at $\alpha_{\text{HF}}=0.25$ (Fig.1, central panel). Importantly, the Cr empty states follow the blue shift of the CBM, while the occupied states follow the VBM downward (Fig.1, top panel). Occupied states dive away from the CBM already at low α_{HF} , as expected from self-interaction removal, whereas empty Cr states hardly move with respect to the CBM. In particular, the lowest unoccupied (majority) Cr levels are at about 2.6 eV from CBM at all α_{HF} (thus, the exact value of α_{HF} is not critical).

Empty and occupied Cr-states separate drastically, from 2.2 eV in GGA to 7 eV in HSE06 (Fig.1, bottom panel). This separation is experimentally unknown in $\text{Cr}:\text{In}_2\text{O}_3$ but it was measured from combined X-ray photoemission and Bremsstrahlung spectroscopy [21] to be around 6 eV for Cr_2O_3 , where Cr is also trivalent and octahedrally coordinated. We reproduced that value for Cr_2O_3 at $\alpha_{\text{HF}}=0.25$, providing an independent countercheck of, and support to, the HSE06 recipe.

To complete the picture, we study Cr_b by the GGA+U method, with Hubbard parameters set as in the GGA+U/NLEP calculation [5]. As shown in Fig.1 (right panels), GGA+U yields a gap of 1.27 eV, less than half the experimental value. This is not surprising because the relative orbital and spin polarization of the gap-edge states (respectively, small and non-existent) offer limited leverage to the U correction. Occupied Cr-induced levels are placed by GGA+U at 0.5 eV above the VBM, and empty states $\simeq 2$ eV above the CBM. Overall, these results are roughly similar to HSE with $\alpha_{\text{HF}}\sim 0.1$. Comparison with GGA+U/NLEP results (reported in the same Figure) indicates that the CBM is shifted with respect to the dopant potential by the NLEP corrections, keeping the Cr-levels close to the conduction band edge while the gap is opened up. (The NLEP gap was tuned [5] to the optical onset of 3.5 eV, rather than to the lowest dipole-forbidden gap of 2.9 eV [15]. HSE at $\alpha_{\text{HF}}=0.25$, in turn, gives both gaps in agreement with experiment.)

We now consider the implications of the result for carrier-mediated FM. In Ref.5, empty minority Cr e_g levels are sufficiently close in energy to the CBM so as to be occupied by free carriers (density 10^{21} cm^{-3}) provided e.g. by shallow donors, and thus produce itinerant FM à la diluted-magnetic-semiconductors. Our results indicate instead that carrier-mediated FM cannot result from

doping occupation of Cr-induced states in the presence of Cr alone. Empty Cr states are over 2.5 eV above the CBM, so that their filling by electrons provided by In-substitutional bond-saturating shallow donors such as Sn is impossible, as the Fermi level cannot rise so high even at high Sn concentrations. We verified by calculations that Sn, as expected of a shallow donor, hardly modifies the band structure and just induces a near-CBM shallow level (effectively, a lowering of the CBM by 40 meV at 3.1% Sn) which does not hybridize or interact with any Cr levels. Thus, the free carriers do not interact with either the occupied or the empty Cr levels, and we are led to conclude that FM cannot be sustained in In_2O_3 by Cr alone at any plausible doping level.

To make progress, we note that experiments [1, 2] indicate unambiguously that FM occurs in $\text{Cr}:\text{In}_2\text{O}_3$ only for oxygen-lean growth conditions (i.e. low oxygen pressure) or after high-vacuum annealing. In fact, this makes it easier to achieve FM in practice, as O loss upon cooling is endemic in this material. FM is however suppressed entirely (see especially Fig.3c of Ref.1) at large O pressures or after O-rich annealing. It is thus natural to suppose that defects related to oxygen deficiency be involved in establishing magnetic coupling (as e.g. in the case of Co in ZnO [22]). As a minimal sample of such defects, we study the isolated vacancy V_{O} and the $\text{Cr}_b\text{-}V_{\text{O}}$ complex in their neutral state; the relevant doping is n -type, so vacancy deep donors never charge positively. We assume, by computational necessity, concentrations of 2% and 3% respectively for V_{O} and Cr, i.e. one vacancy and one Cr per simulation cell (density of $9 \times 10^{20} \text{ cm}^{-3}$ each).

The isolated vacancy gives rise to a moderately dispersed mid-gap fully occupied and non-spin-polarized extrinsic level, made up from the totally-symmetric combination of In dangling states. On the other hand, the $\text{Cr}_b\text{-}V_{\text{O}}$ complex –i.e. the vacant site with one Cr and three In neighbors– has two spin-split occupied gap states, one of Cr-In character in the majority channel (about 25% Cr), and one purely In-like in the minority, as shown in Fig.2, left panel. The majority state is lower in energy across the whole Brillouin zone, due to Hund’s coupling with Cr t_{2g} majority states. So, due to on-site exchange splitting, Cr majority states are de facto the only ones available. Both the minority and majority vacancy gap states are filled, so the magnetic moment remains the $3 \mu_B$ of the Cr t_{2g} core.

The HSE electronic structure turns out to be conducive to long-range magnetic coupling with features compatible with experiment, as we will discuss momentarily. Before that, we briefly note that the GGA+U band structure in Fig.2, right panel, suggests a different picture (erroneously, by comparison with HSE): due to the smaller gap, more dispersed vacancy states, and artificially stronger coupling of e_g and occupied t_{2g} , a heavily Cr-like polarized state drops in energy and becomes fully occupied, while a mixed Cr-In doublet hosts the second

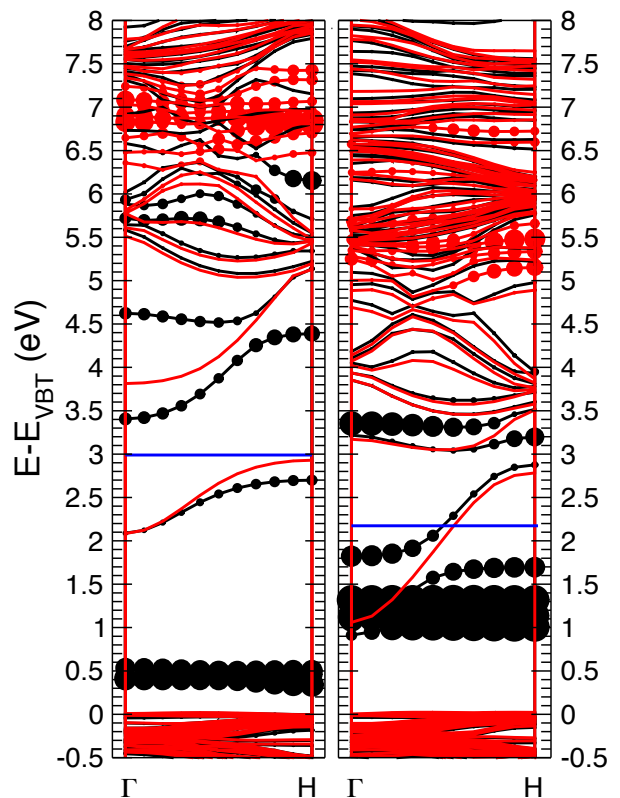


FIG. 2. (Color online) HSE (left) and GGA+U (right) band structure of the $\text{Cr}_b\text{-}V_{\text{O}}$ complex. Majority states are black, minority are red (gray). Size of dots is proportional to projection on Cr. Energy zero in both panels is valence band edge. Horizontal line is the Fermi energy.

electron and remains half-occupied; the saturation moment is $4 \mu_B$, and the partially occupied polarized states imply doping-independent itinerant coupling, contrary to experimental results.

Let us go back to the HSE electronic structure. The spectrum is gapped, and the occupied states cannot provide itinerant coupling; thus, in the absence of doping the system is paramagnetic. However, the Cr-induced spin-polarization propagates to conduction band states (Fig.2, left panel), i.e. these states are now significantly Cr-like and spin-polarized, *and* within reach of intentional or accidental doping. Charge added into these states will be delocalized and polarized, and will produce an itinerant coupling between neighboring Cr centers. In nominally undoped material, the experimental net magnetization is zero or at most a few percent ($0.1 \mu_B$) of the expected $3 \mu_B/\text{Cr}$; this can be understood as a result of unintentional doping, or of impurity band formation due to a large V_{O} excess over Cr (quite typical in experiment). Upon intentional shallow-donor doping, the experimental magnetization increases significantly (up to $1.5 \mu_B$ or so), but always falls short of the saturation value. In our picture, this increase should occur as the electron

density is raised up to $1.5 \div 2 \times 10^{21} \text{ cm}^{-3}$, whereby only the majority Cr CBM state is occupied (estimated using a free-electron-like density of states and assuming rigid-band behavior). This matches roughly the typical 2:1 ratio of free-electron to Cr concentration in FM samples [1]. Above that density, the minority state will progressively fill up and compensate the majority. While it proved computationally impossible to calculate directly the magnetic coupling and critical temperature at this Cr density, it is virtually guaranteed that the itinerant coupling will be FM, and not antiferromagnetic, given the plethora of available states for FM hopping in the standard virtual-superexchange picture. We note in closing that this picture partly resembles the earlier one [5], with the key difference that the Cr- V_O complex must be present to bring e_g -like states within reach of doping.

We observe that Cr_i and V_O which are not first neighbors do not interact: their electronic structure resembles the superposition of those of the isolated defects. Cr- V_O is thus the effective magnetic-dopant unit in this system, and should be energetically bound to act as such, i.e. its binding energy

$$B = |E_{Cr-V_O} + E_{\text{bulk}}| - |E_{Cr} + E_{V_O}|$$

should be positive. Here the E 's are the energies of a supercell containing, respectively, the Cr- V_O complex, no defect at all, and each of the two isolated defects. At the In_2O_3 equilibrium volume and equal Cr and V_O densities, $B \simeq 0$ to numerical accuracy, implying roughly equal populations of Cr-V complexes and isolated Cr; such a situation would be already sufficient to cause itinerant magnetism. Interactions of Cr with a very large vacancy density (possibly via multivacancy-Cr complexes, local structure, bonding, and impurity band formation) may play a stabilizing role; this cannot be assessed directly, as it would require a configurational sampling of vacancy and Cr configurations at several vacancy densities, which is computationally prohibitive. We investigated the effect of volume reduction, as would occur at high oxygen deficiency via the negative vacancy formation volume, and found that B is insensitive to it.

Aside from the binding, O-rich growth conditions or oxidizing post-processing will suppress the magnetic coupling (as consistently observed [1, 2]) by annihilating vacancies and hence Cr- V_O 's. As mentioned, though, normal handling of In_2O_3 , such as cooling in air, is effectively reducing, so O deficiency will generally be realized.

In summary, the electronic structure of isolated Cr in In_2O_3 as provided by hybrid density functionals is not compatible with ferromagnetism. We proposed an alternative mechanism enabled by Cr- V_O complexes and boosted by intentional doping, which is consistent with experimental results such as the low net moment in unintentionally doped material, FM onset only in O-lean conditions, and moment increase upon intentional doping.

Work supported in part by MIUR-PRIN 2010 project *Oxide*, Fondazione Banco di Sardegna and CINECA-ISCRA grants. MC thanks M. Martino and A. P. Caricato for their support and assistance in the early stages of this work. This paper is based in part on portions of the PhD thesis presented by MC at University of Salento, Lecce, Italy, in 2012.

-
- [1] J. Philip, A. Punnoose, B.I. Kim, K.M. Reddy, S. Layne, J.O. Holmes, B. Satpati, P.R. Leclair, T.S. Santos and J.S. Moodera, *Nature Materials* **5**, 298 (2006).
 - [2] F. X. Jiang, X. Hu, J. Zhang, X. C. Fan, H. S. Wu and G. A. Gehring, *Appl. Phys. Lett.* **96**, 052503 (2010); G. Z. Xing, J. B. Yi, D. D. Wang, L. Liao, T. Yu, Z. X. Shen, C. H. A. Huan, T. C. Sum, J. Ding and T. Wu, *Phys. Rev B* **79**, 174406 (2009); R. P. Panguluri, P. Kharel, C. Sudakar, R. Naik, R. Suryanarayanan, V. M. Naik, A. G. Petukhov, B. Nadgorny and G. Lawes, *Phys. Rev. B* **79**, 165208 (2009); R. Naik and V. M. Naik. *J. Appl. Phys.* **101**, 09H117 (2007).
 - [3] T. Dietl, *Nature Materials* **2**, 646 (2003); T. Dietl, H. Ohno, F. Matsukura, J. Cibert and D. Ferrand, *Science* **287**, 1019 (2000); H. Ohno, *Science* **281**, 951 (1998); J. K. Furdyna, *J. Appl. Phys.* **64**, R29 (1988).
 - [4] L. M. Huang, C. Moyses Araujo and R. Ahuja, *EPL* **87**, 27013 (2009).
 - [5] H. Raebiger, S. Lany and A. Zunger, *Phys. Rev. Lett.* **101**, 027203 (2008); *ibidem*, *Phys. Rev. B* **79**, 165202 (2009).
 - [6] S. Lany, H. Raebiger and A. Zunger, *Phys. Rev. B* **77**, 241201(R) (2008); S. Lany and A. Zunger, *Modelling Simul. Mater. Sci. Eng.* **17**, 084002 (2009).
 - [7] J. Heyd, G. E. Scuseria, and M. Ernzerhof, *J. Chem. Phys.* **118**, 8207 (2003).
 - [8] J. P. Perdew, K. Burke, and M. Ernzerhof, *Phys. Rev. Lett.* **77**, 3865 (1996).
 - [9] A. Stroppa and G. Kresse, *Phys. Rev. B* **79**, 201201 (2009).
 - [10] P. Alippi, F. Filippone, G. Mattioli, A. Amore Bonapasta, and V. Fiorentini, *Phys. Rev. B* **84**, 033201 (2011).
 - [11] P.E. Blöchl, *Phys. Rev. B* **50**, 17953 (1994); G. Kresse, and D. Joubert, *Phys. Rev. B* **59**, 1758 (1999).
 - [12] G. Kresse and J. Hafner, *Phys. Rev. B* **47**, 558 (1993); G. Kresse and J. Furthmüller, *Comput. Mater. Sci.* **6**, 15 (1996); *Phys. Rev. B* **54**, 11169 (1996).
 - [13] M. Marezio, *Acta Crystallogr.* **20**, 723 (1966). J. Hafner, *J. Comp. Chem.* **29**, 2044 (2008).
 - [14] A. Walsh, J. L. F. Da Silva and S.-H. Wei, *Phys. Rev. B* **78**, 075211 (2008); P. Agoston, K. Albe, R. M. Nieminen and M. J. Puska, *Phys. Rev. Lett.* **103**, 245501 (2009); C. Körber, V. Krishnakumar, A. Klein, G. Panaccione, P. Torelli, A. Walsh, J. L. F. Da Silva, S.-H. Wei, R. G. Egdell and D. J. Payne, *Phys. Rev. B* **81**, 165207 (2010).
 - [15] P. D. C. King, T. D. Veal, F. Fuchs, Ch. Y. Wang, D. J. Payne, A. Bourlange, H. Zhang, G. R. Bell, V. Cimalla, O. Ambacher, R. G. Egdell, F. Bechstedt and C. F. McConville, *Phys. Rev. B* **79**, 205211 (2009).
 - [16] V. Christou, M. Etchells, O. Renault, P. J. Dobson, O. V. Salata, *J. Appl. Phys.* **88**, 5180 (2000).

- [17] M. A. Klein, Appl. Phys. Lett. **77**, 2009 (2000) and references therein.
- [18] L. Marsella and V. Fiorentini, Phys. Rev. B **69**, 172103 (2004).
- [19] D. Payne and E. A. Marquis, Chem. Mater. **23**, 1085 (2011).
- [20] R. Wyckoff, *Crystal structures* (J. Wiley, New York, 1963), Vol. 1.
- [21] R. Zimmermann, P. Steiner, and S. Hufner, J. Electr. Spectr. Rel. Phen. **78**, 49 (1996).
- [22] C. D. Pemmaraju, R. Hanafin, T. Archer, H. B. Braun, and S. Sanvito, Phys. Rev. B **78**, 054428 (2008); G. Ciatto, A. Di Trolio, E. Fonda, P. Alippi, A. M. Testa, and A. Amore Bonapasta, Phys. Rev. Lett. **107**, 127206 (2011).